**Supporting information for**

# Platinum(II) Complexes with Novel Diisocyanide Ligands: Catalysts in Alkyne Hydroarylation

*Daniele Vicenzi,*[†] *Paolo Sgarbossa,*[‡*] *Andrea Biffis,*[†] *Cristina Tubaro,*[†*] *Marino Basato,*[†] *Rino A. Michelin,*[‡] *Arianna Lanza,*[†] *Fabrizio Nestola,*[§] *Sara Bogialli,*[†] *Paolo Pastore,*[†] *Alfonso Venzo*[‖]

[†] Dipartimento di Scienze Chimiche, Università di Padova, via Marzolo 1, 35131 Padova.

[‡] Dipartimento di Ingegneria Industriale, Università di Padova, via Marzolo 9, 35131 Padova.

[§] Dipartimento di Geoscienze, Università di Padova, via Gradenigo 6, 35131 Padova.

[‖] IENI-CNR, Dipartimento di Scienze Chimiche, Università di Padova, via Marzolo 1, 35131 Padova.

paolo.sgarbossa@unipd.it (P.S.); cristina.tubaro@unipd.it (C.T.)

**Experimental Section.**

**General remarks**

NMR spectra were recorded at 298 K on a Bruker Avance-III 200 MHz (200.13 MHz for $^{1}H$, 50.32 for $^{13}C$, 81.01 for $^{31}P$) or on a Bruker Avance DX-400 (400.13 MHz for $^{1}H$ and 100.61 for $^{13}C$); chemical shifts (δ) are reported in units of ppm relative to $Si(CH_3)_4$ or the residual solvent signals for $^{1}H$ and $^{13}C$ NMR spectra, and to 85% $H_3PO_4$ for $^{31}P$ NMR spectra. The FT-IR spectra were obtained with a Perkin Elmer Spectrum 100 spectrophotometer, with a resolution of 2 $cm^{-1}$. ESI-MS analyses were performed using a LCQ-Duo (Thermo-Finnigan) operating in positive ion mode. Instrumental parameters: capillary voltage 10 V, spray voltage 4.5 kV; capillary temperature 200 °C; mass scan range from 150 to 2000 amu; $N_2$ was used as sheath gas; the He pressure inside the trap was kept constant. The pressure directly read by an ion gauge (in the absence of the $N_2$ stream) was $1.33 \times 10^{-5}$ Torr. Sample solutions were prepared by dissolving the compounds in acetonitrile. Sample solutions were directly infused into the ESI source by a syringe pump at 8μL/min flow rate. Liquid chromatography (LC)-high resolution MS (HRMS) analyses were performed with an UHPLC system (Agilent Series 1200; Agilent Technologies, Palo Alto, CA, USA), consisting of vacuum degasser, auto-sampler, a binary pump coupled to a Quadrupole-Time of Flight mass analyzer (Agilent Series 6520; Agilent Technologies) with an ESI source, using nitrogen gas and operating in positive acquisition, with the following operation parameters: capillary voltage, 3500 V; nebulizer pressure, 35 psi; drying gas, 8 L $min^{-1}$; gas temperature, 350°C; fragmentor voltage in the range of 80-200 V; skimmer 65 V.

Analyses were performed injecting a total of 40 μL (8 X 5μL injection volume) of samples by means of an injection program, varying each time the fragmentor voltage. The mobile phase was acetonitrile or acetonitrile 0.1 % HTFA at flow rate of 0.2 mL $min^{-1}$. Full scan mass spectra were recorded as centroid over the 50–3000 m/z range with a scan rate of 2 spectra/s. Mass spectra acquisition and data analysis was processed with Masshunter Workstation B 04.00 software (Agilent Technologies).

**Table S1.** Selected crystallographic data for complexes **2**, **1'** and **2'**

| Complex | **2** | **1'** | **2'** |
|---|---|---|---|
| Formula | $C_{22}$ $H_{12}$ $Cl_2$ $N_2$ $O_4$ Pt | $C_{22}$ $H_{19}$ $N_2$ $O_3$ P Pt | $C_{48}H_{36}N_4O_8Pt_2 \cdot CH_2Cl_2$ |
| Molecular weight | 634.33 | 585.45 | 1271.91 |
| Crystal system | Monoclinic | Monoclinic | Monoclinic |
| Space group | $P2_1/c$ | $P2_1/n$ | C 2/c |
| *a*/Å | 14.7441(14) | 11.871(1) | 26.097(4) |
| *b*/Å | 8.6683(8) | 8.358(1) | 12.1200(14) |
| *c*/Å | 16.881(3) | 21.583(2) | 20.158(3) |
| α/° | 90.00 | 90.00 | 90.00 |
| β/° | 98.386(14) | 93.142(5) | 130.299(9)° |
| γ/° | 90.00 | 90.00 | 90.00 |
| Volume, Å$^3$ | 2134.4(5) | 2138.2(4) | 4862.8(13) |
| *Z* | 4 | 4 | 4 |
| $D_{calc}$/g cm$^{-3}$ | 1.974 | 1.819 | 1.737 |
| F(000) | 1208 | 1128 | 2456 |
| μ(Mo-Kα)/mm$^{-1}$ | 6.857 | 6.66 | 5.91 |
| Reflections collected | 42931 | 40575 | 49583 |
| Unique reflections | 4652 | 3976 | 5306 |
| Observed reflections [I>2$\sigma$(*I*)] | 3468 [$R_{int}$ = 0.047] | 3368 [$R_{int}$ = 0.027] | 3170 [$R_{int}$ = 0.078] |
| *R* [*I* > 2$\sigma$(*I*)] | $R_1$(F) = 0.0308, $wR_2$(F$^2$) = 0.0318 | $R_1$(F) = 0.0290, $wR_2$(F$^2$) = 0.0720 | $R_1$(F) = 0.0507, $wR_2$(F$^2$) = 0.0504 |
| *R* [all data] | $R_1$(F) = 0.0677, $wR_2$(F$^2$) = 0.0363 | $R_1$(F) = 0.0369, $wR_2$(F$^2$) = 0.0763 | $R_1$(F) = 0.1421, $wR_2$(F$^2$) = 0.0645 |
| Goodness of fit on F$^2$ | 0.990 | 1.053 | 1.059 |

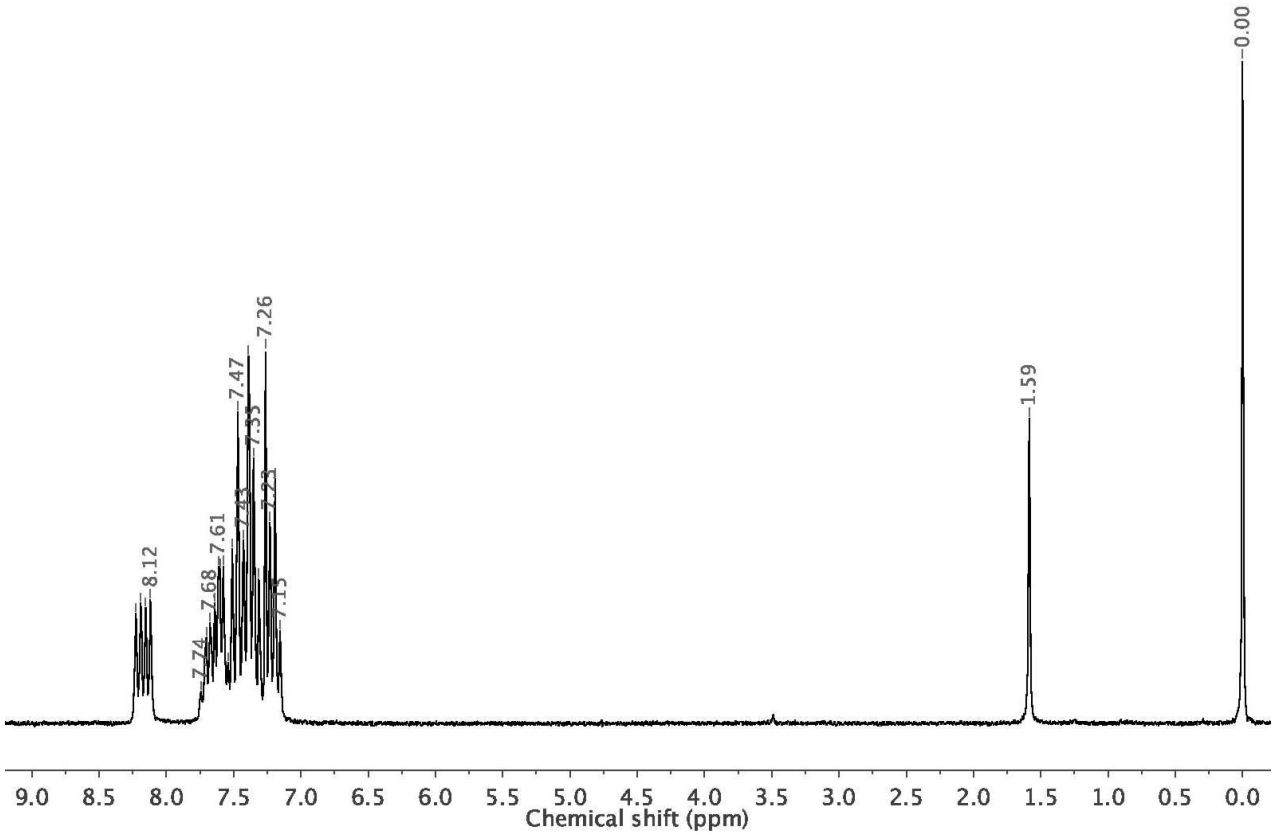


**Figure 1S**. $^{1}H$ NMR spectrum of diNC-1 in $CDCl_3$.

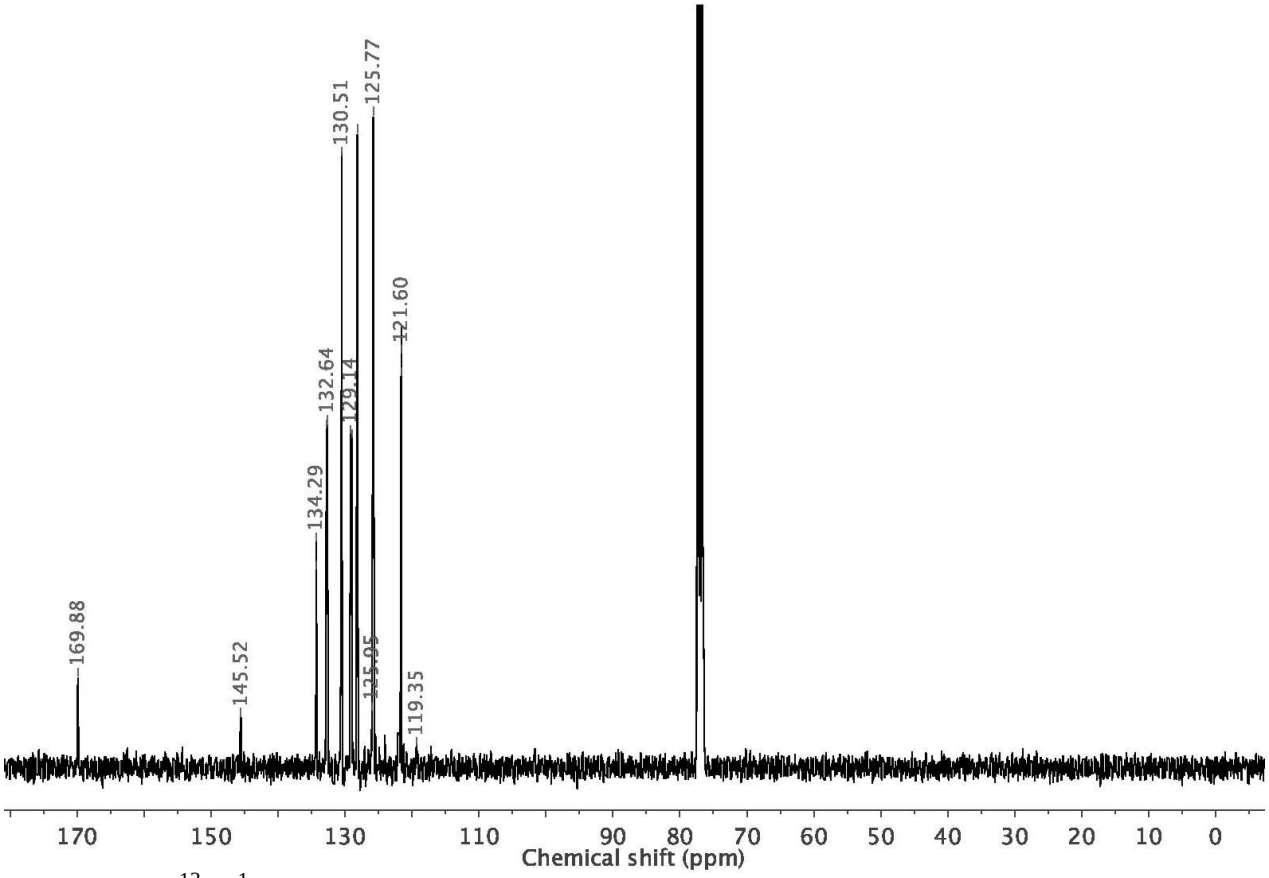


**Figure 2S**. $^{13}C\{^{1}H\}$ NMR spectrum of diNC-1 in $CDCl_3$.

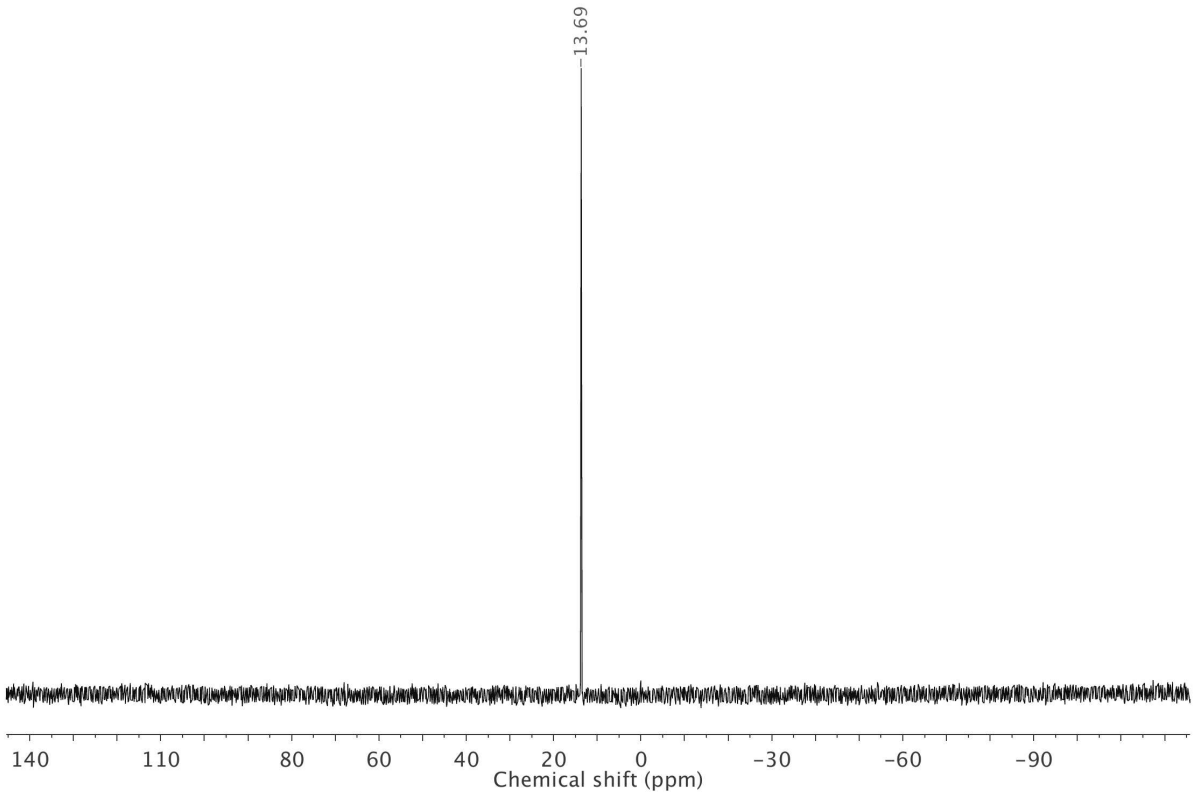


**Figure 3S**. $^{31}P\{^{1}H\}$ NMR spectrum of diNC-1 in $CDCl_3$.

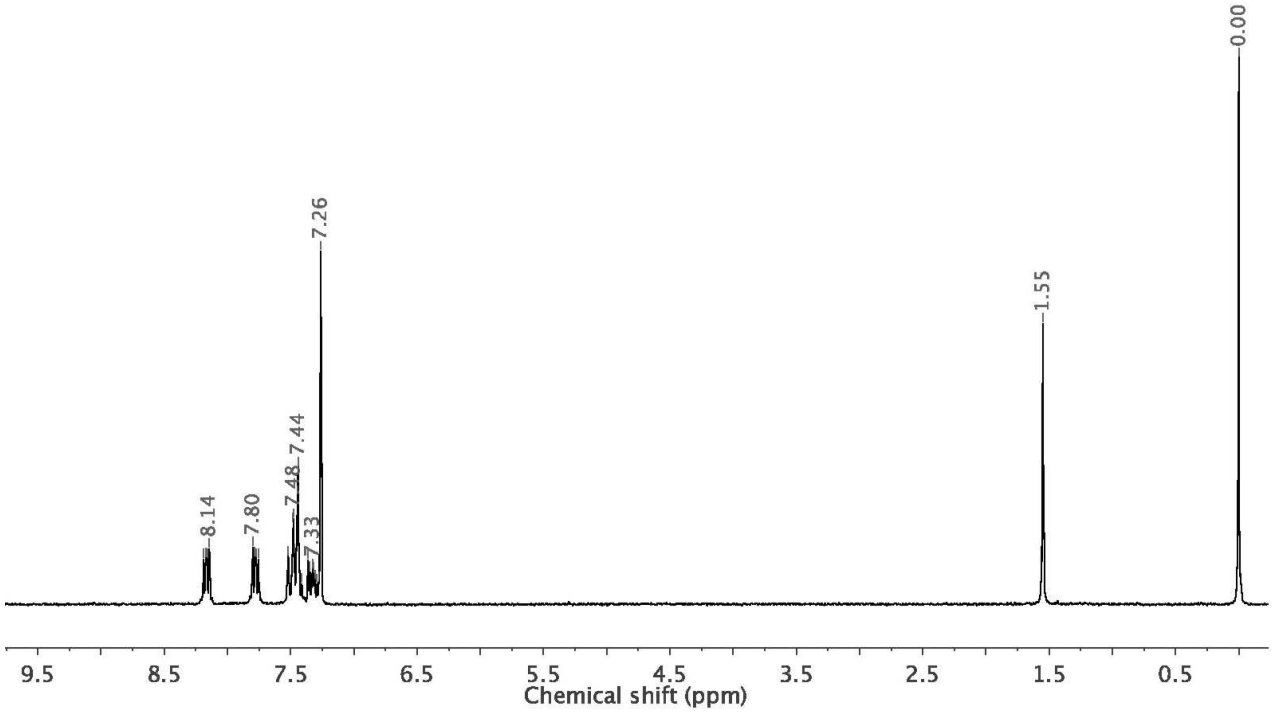


**Figure 4S**. $^{1}H$ NMR spectrum of diNC-2 in $CDCl_3$.

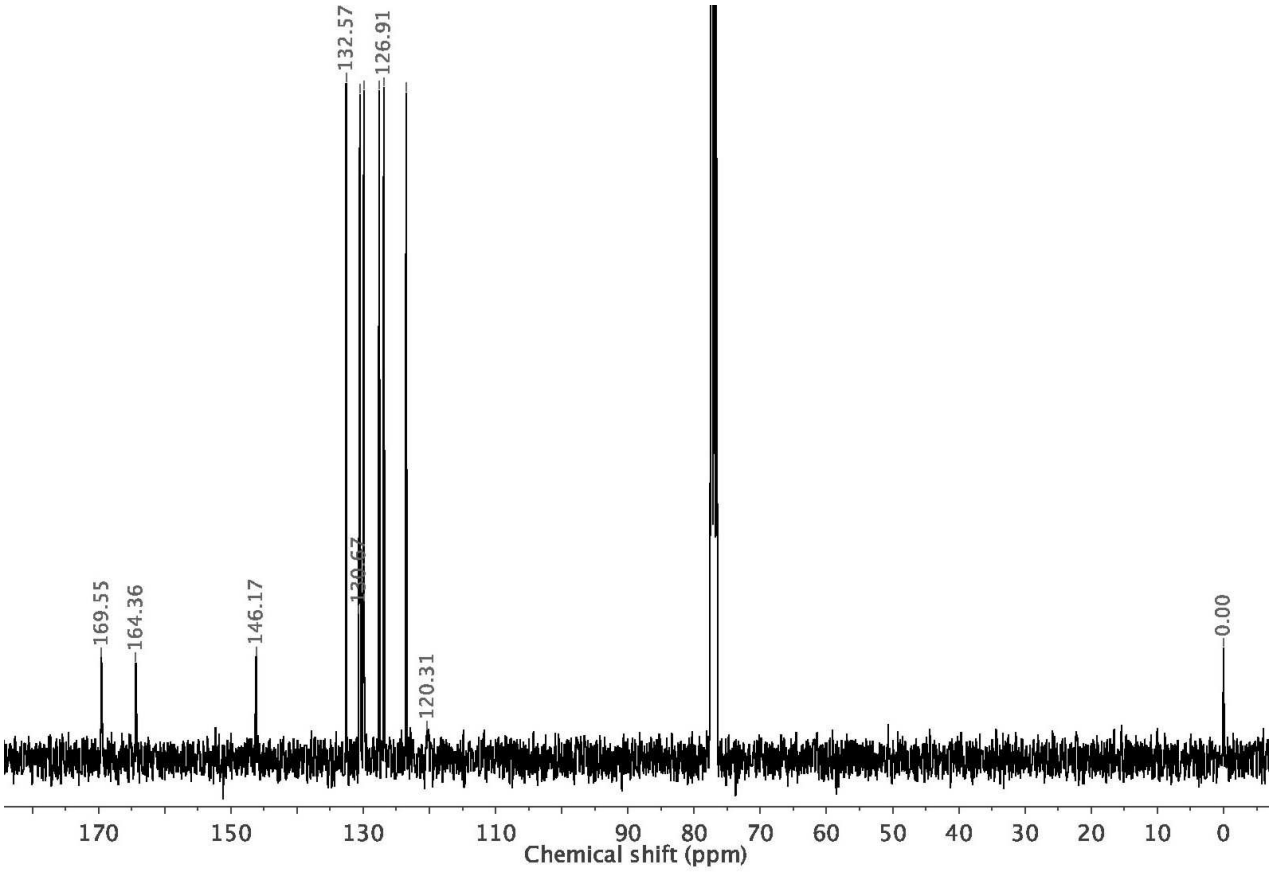


**Figure 5S**. $^{13}C\{^{1}H\}$ NMR spectrum of diNC-2 in $CDCl_3$.

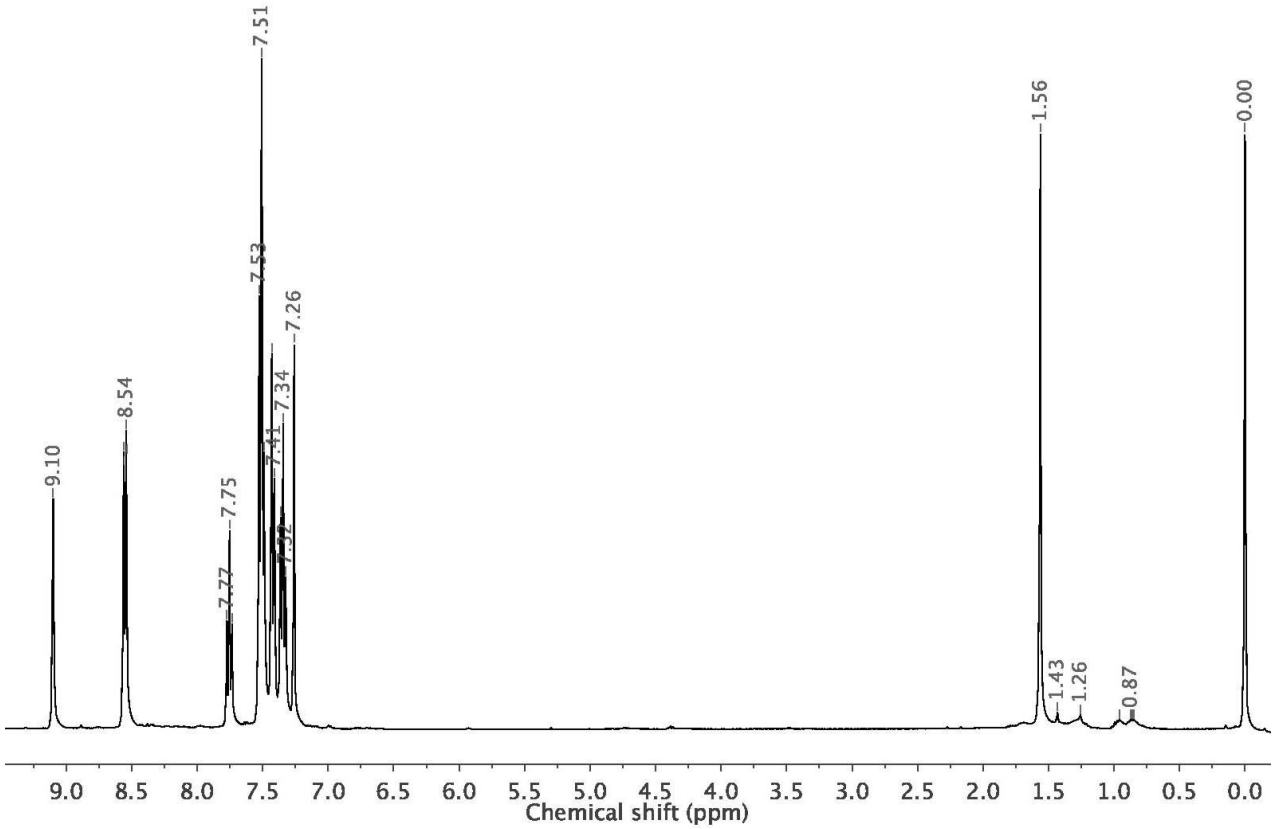


**Figure 6S**. $^{1}H$ NMR spectrum of diNC-3 in $CDCl_3$.

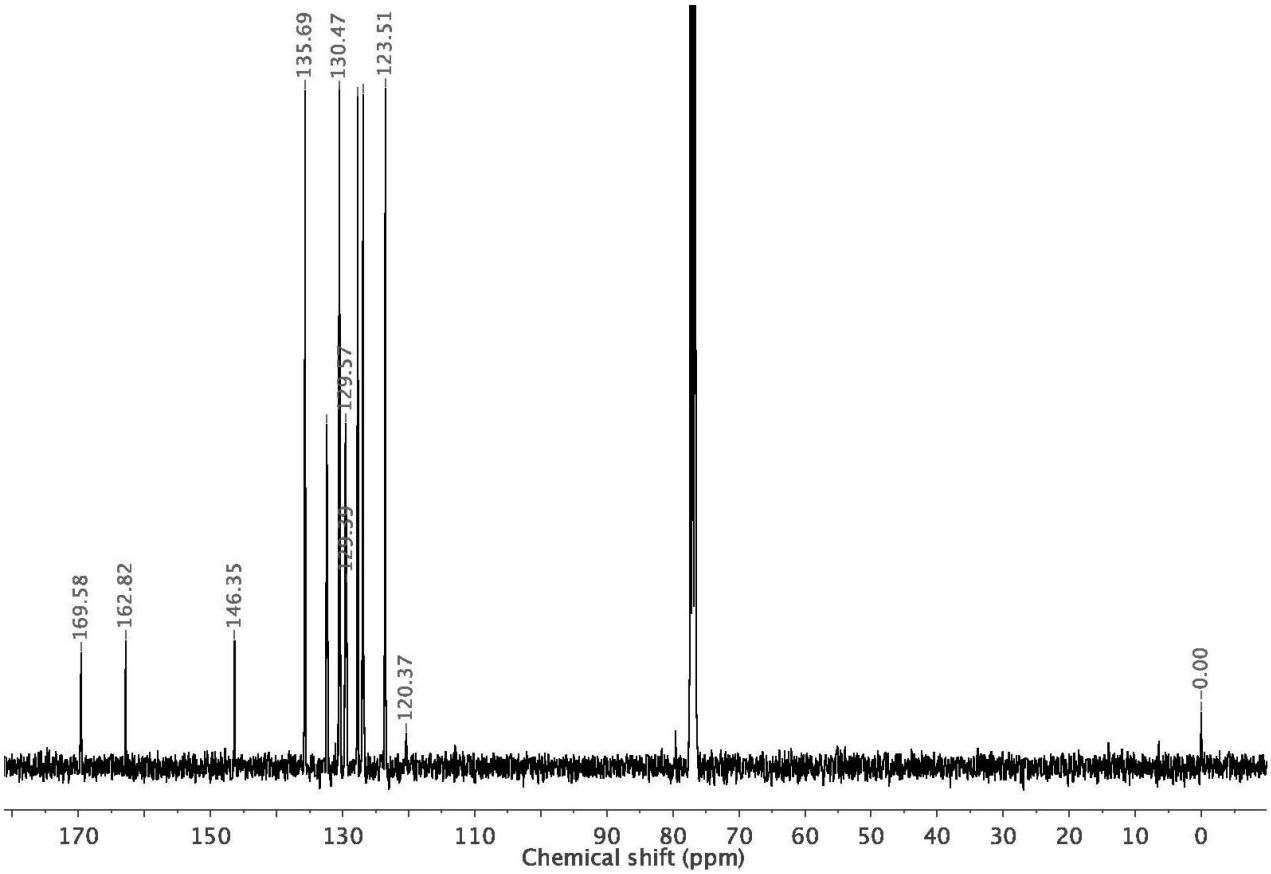


**Figure 7S**. $^{13}C\{^{1}H\}$ NMR spectrum of diNC-3 in $CDCl_3$.

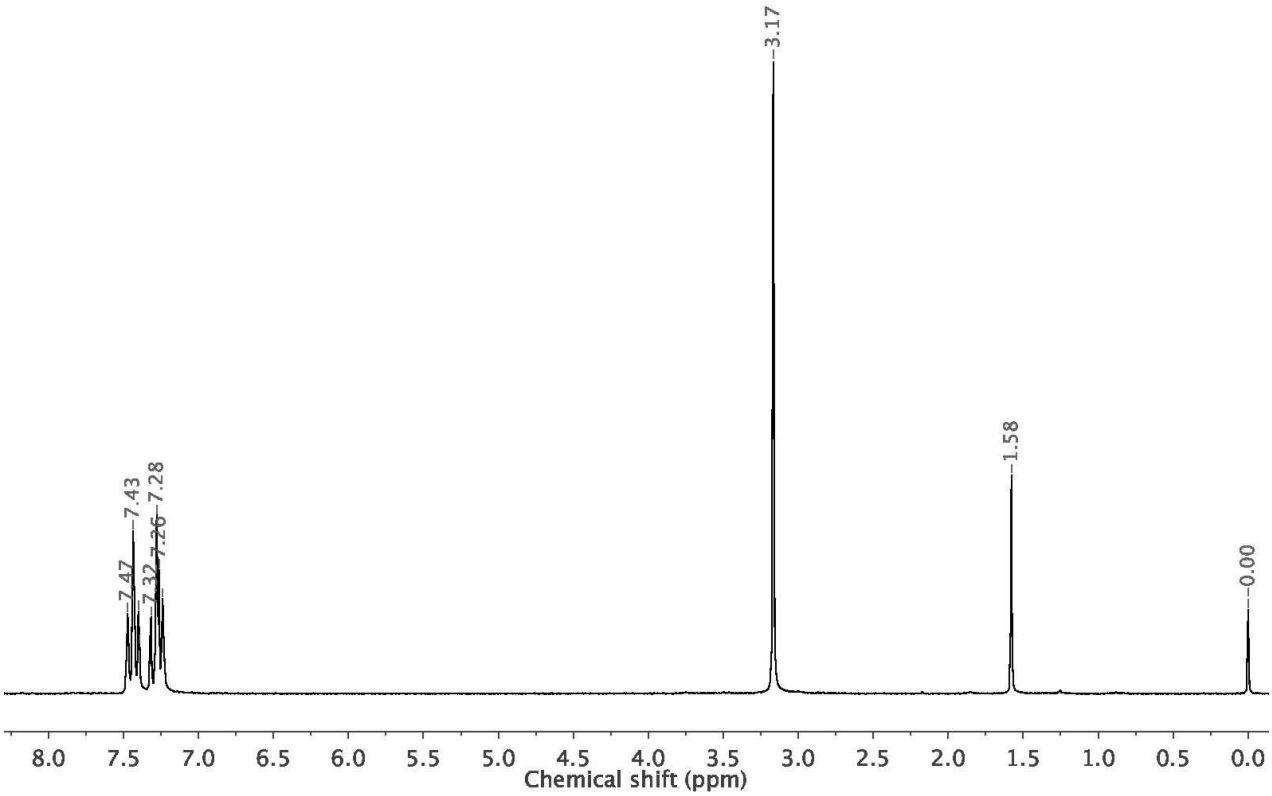


**Figure 8S**. $^{1}H$ NMR spectrum of diNC-4 in $CDCl_3$.

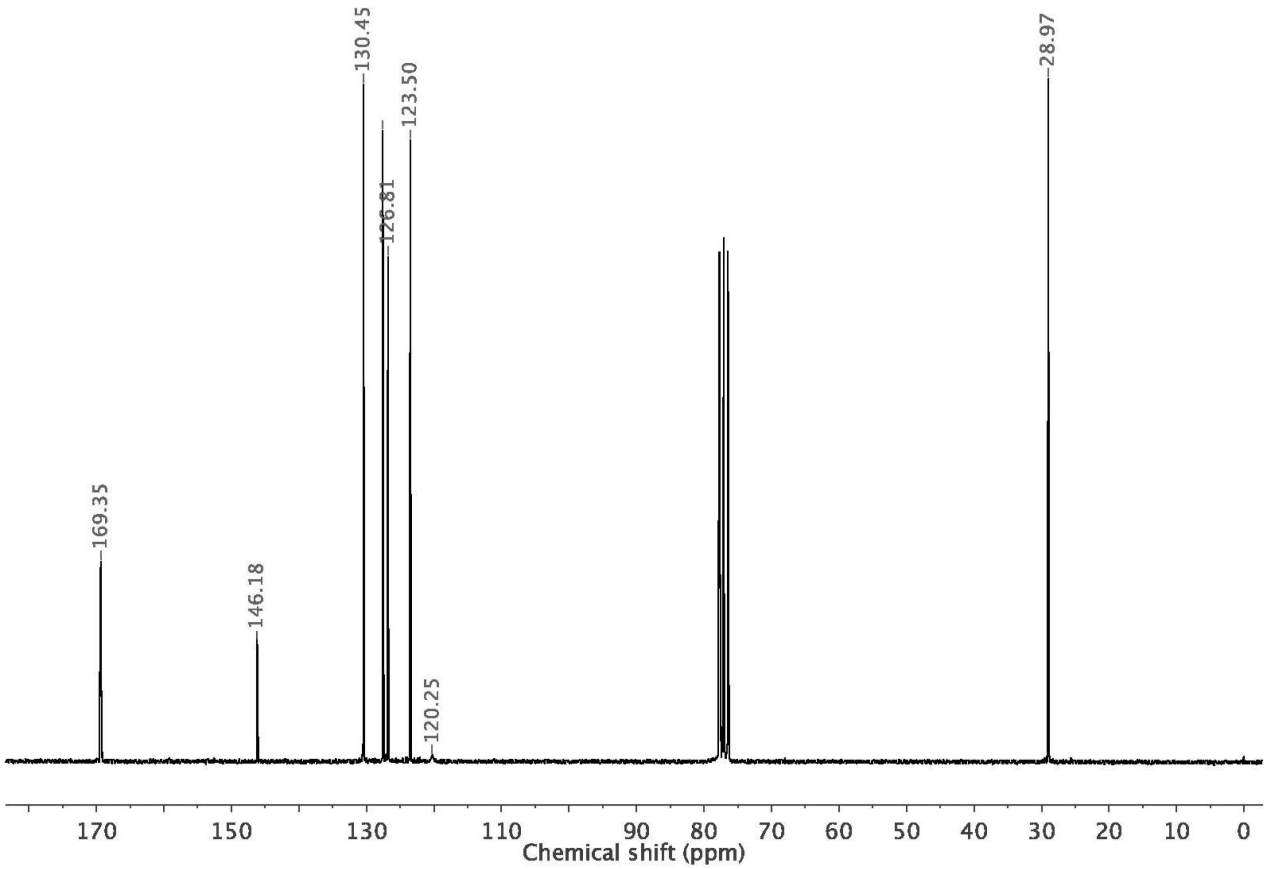


**Figure 9S**. $^{13}C\{^{1}H\}$ NMR spectrum of diNC-4 in $CDCl_3$.

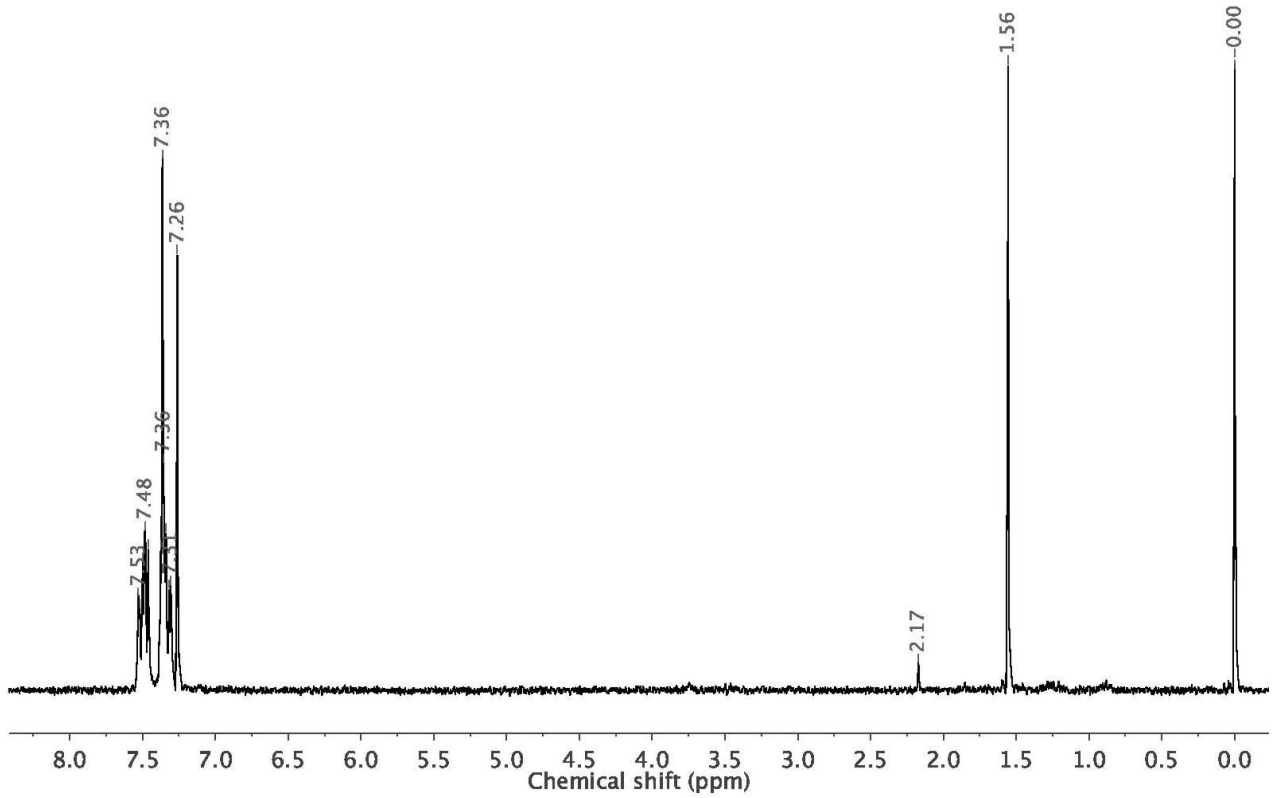


**Figure 10S**. $^{1}H$ NMR spectrum of diNC-5 in $CDCl_3$.

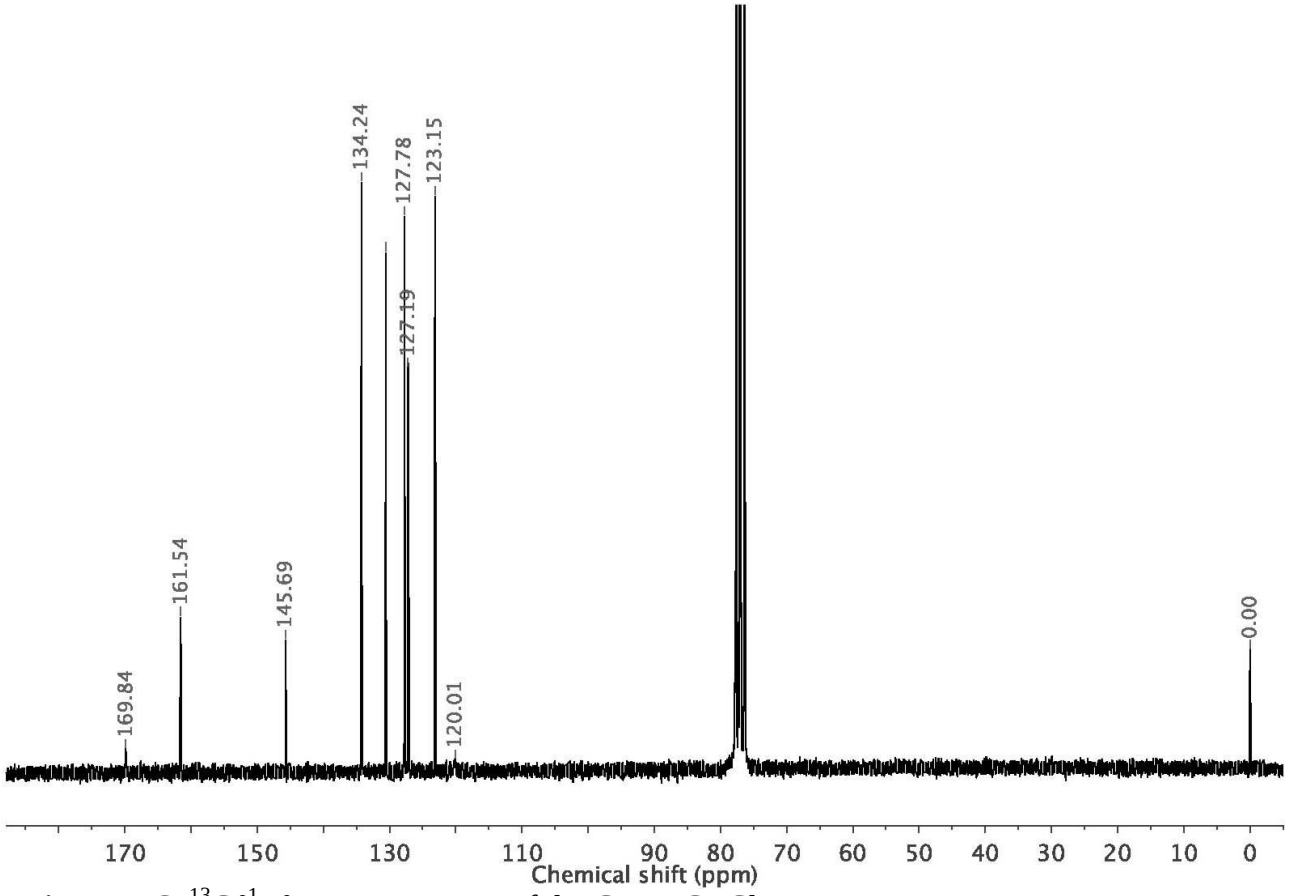


**Figure 11S**. $^{13}C\{^{1}H\}$ NMR spectrum of diNC-5 in $CDCl_3$.

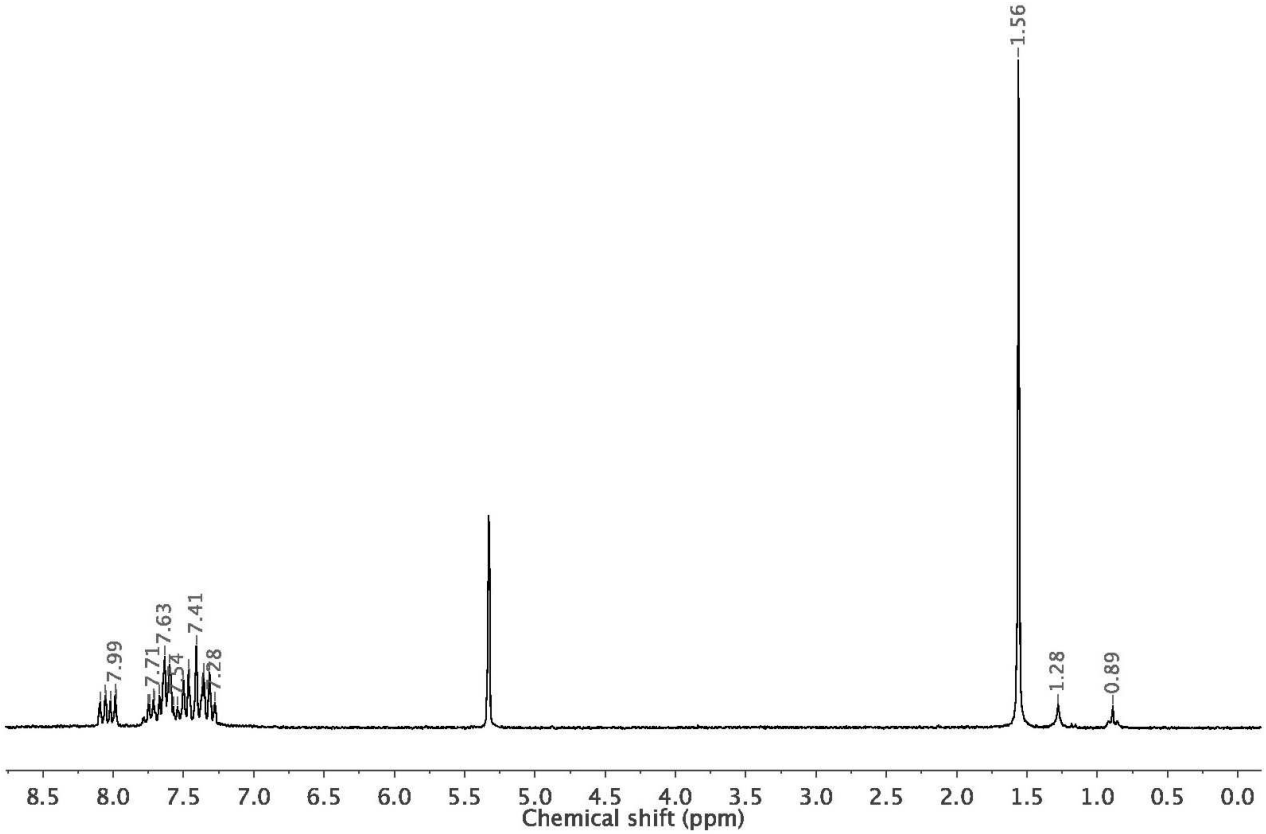


**Figure 12S**. $^{1}H$ NMR spectrum of complex [$PtCl_2$(diNC-1)] (**1**) in $CD_2Cl_2$.

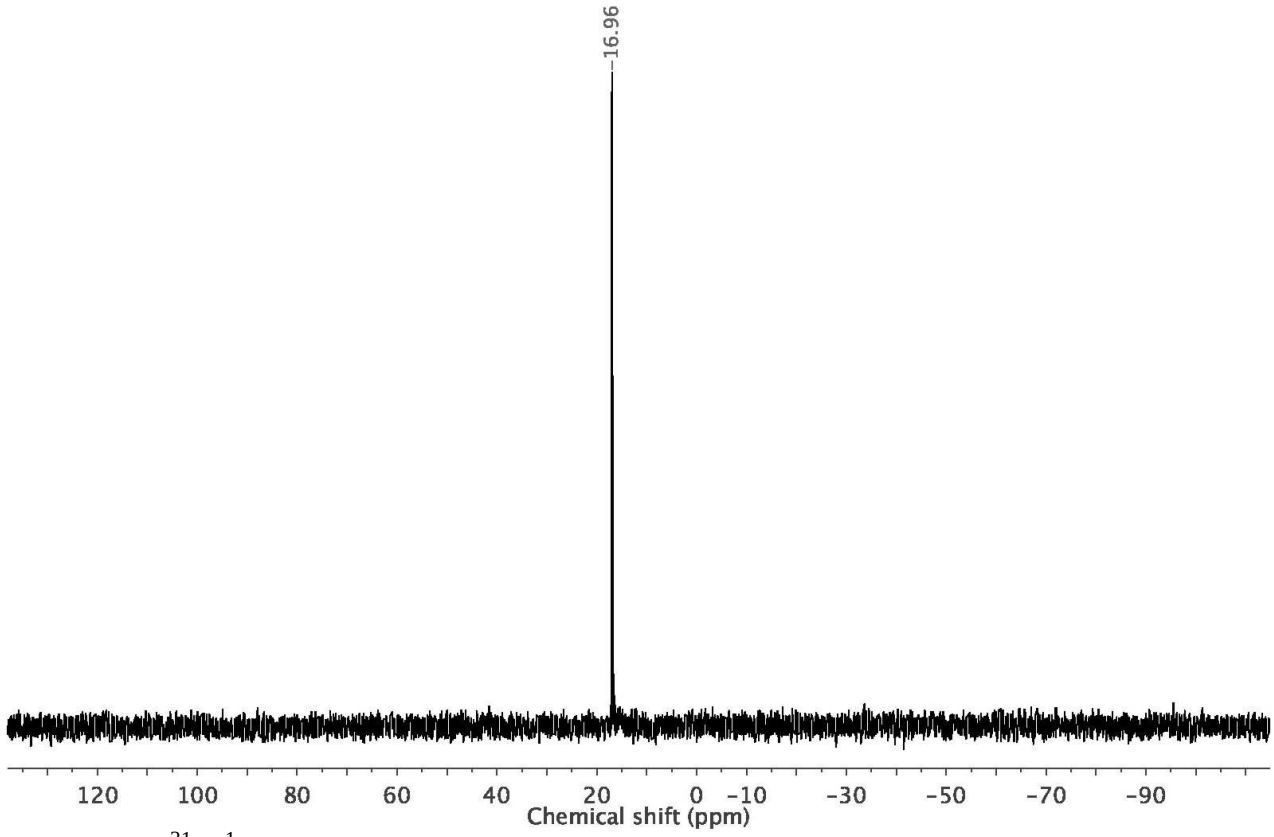


**Figure 13S**. $^{31}P\{^{1}H\}$ NMR spectrum of complex [$PtCl_2$(diNC-1)] (**1**) in $CD_2Cl_2$.

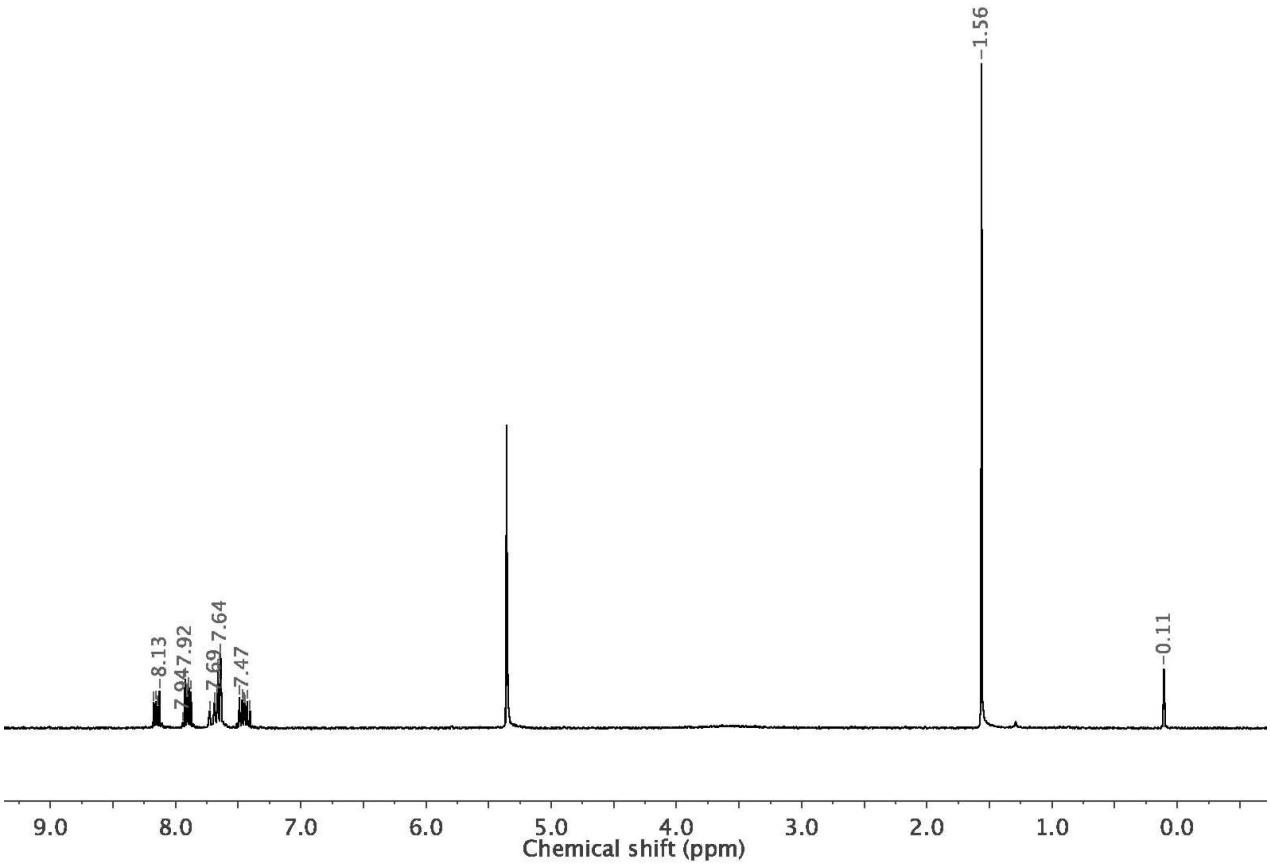


**Figure 14S**. $^{1}$H NMR spectrum of complex [$PtCl_2$(diNC-2)] (**2**) in $CD_2Cl_2$.

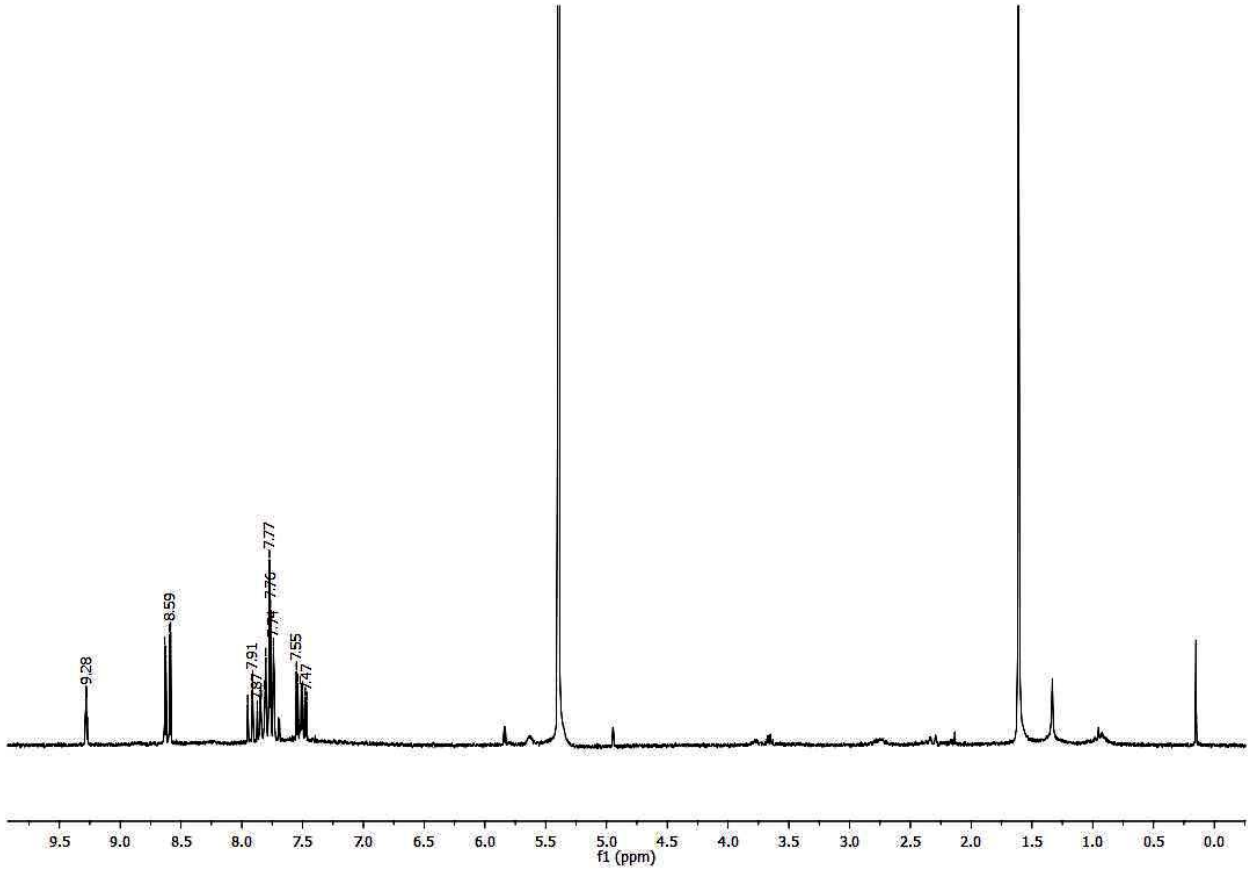


**Figure 15S**. $^{1}$H NMR spectrum of complex [$PtCl_2$(diNC-3)] (**3**) in $CD_2Cl_2$.

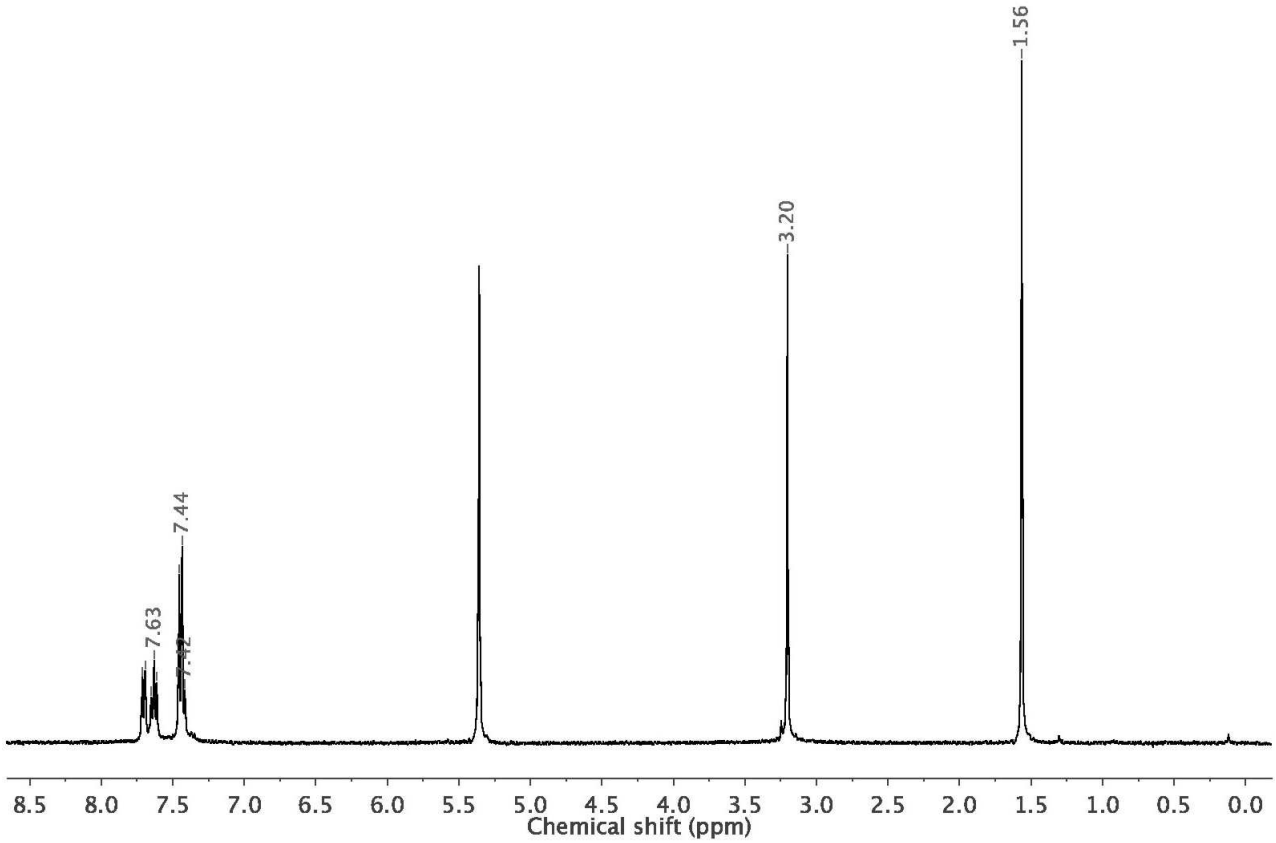


**Figure 16S**. $^{1}H$ NMR spectrum of complex [$PtCl_2$(diNC-4)] (**4**) in $CD_2Cl_2$.

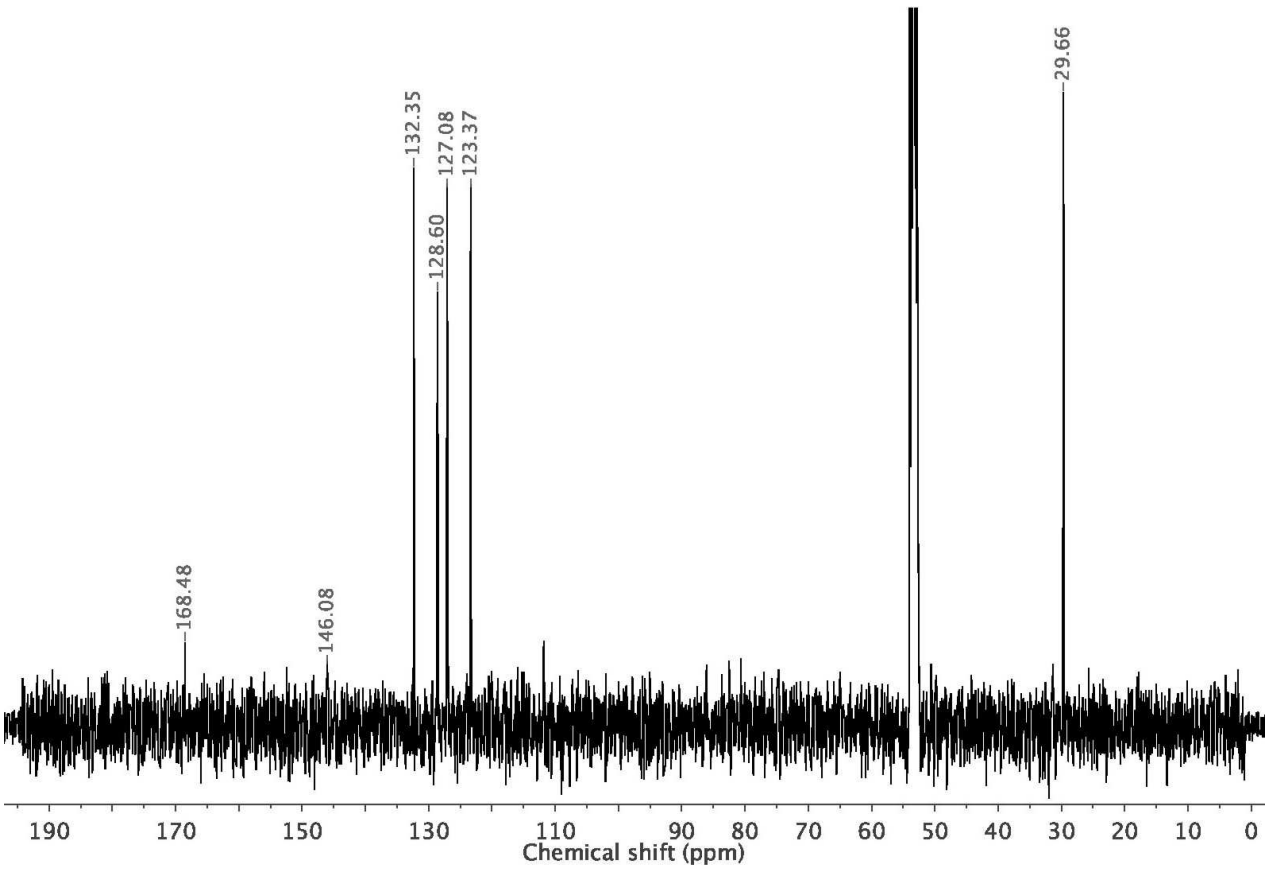


**Figure 17S**. $^{13}C\{^{1}H\}$ NMR spectrum of complex [$PtCl_2$(diNC-4)] (**4**) in $CDCl_3$.

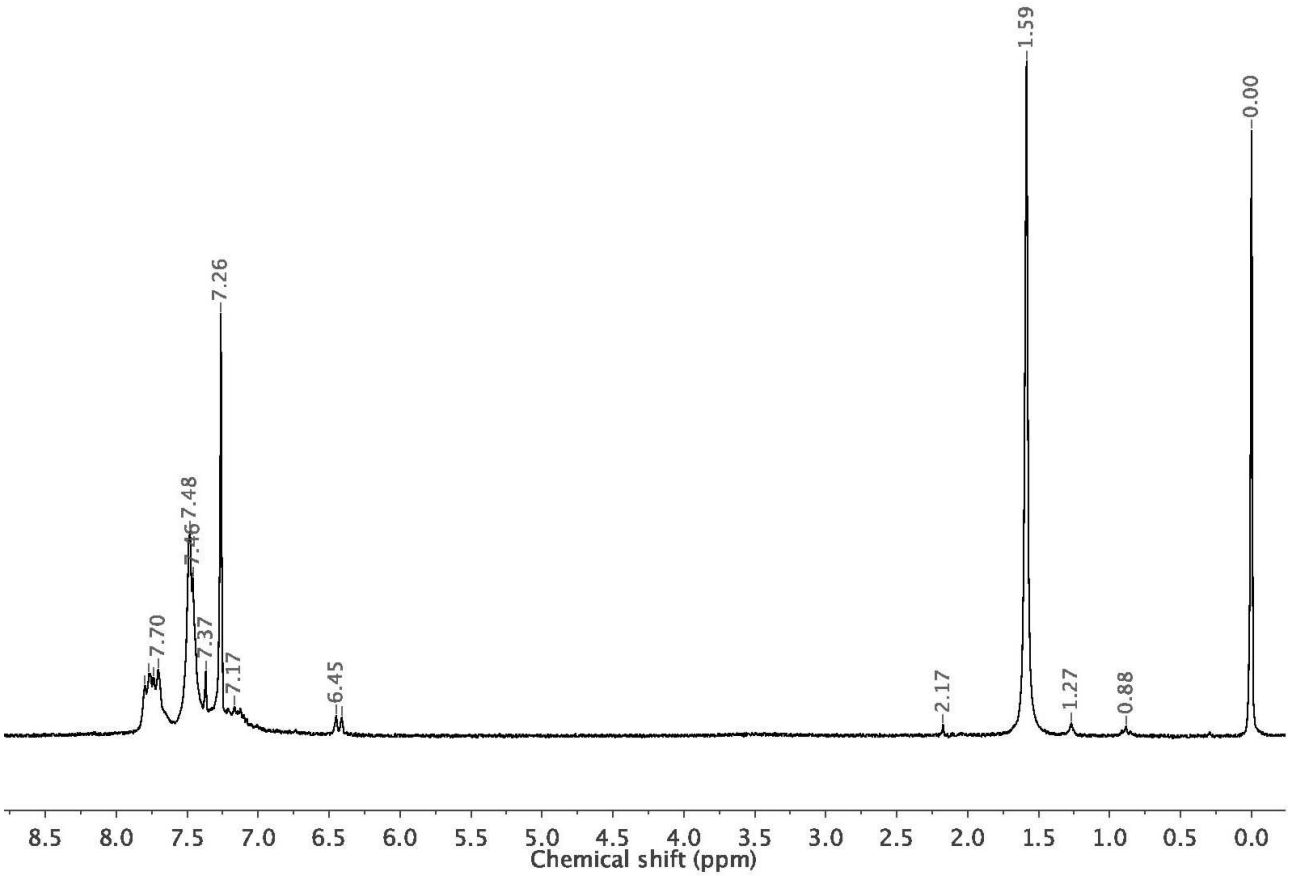


**Figure 18S**. $^{1}H$ NMR spectrum of complex [(μ-diNC-5){$PtCl_2(PPh_3\}_2$] (**5**) in $CDCl_3$.

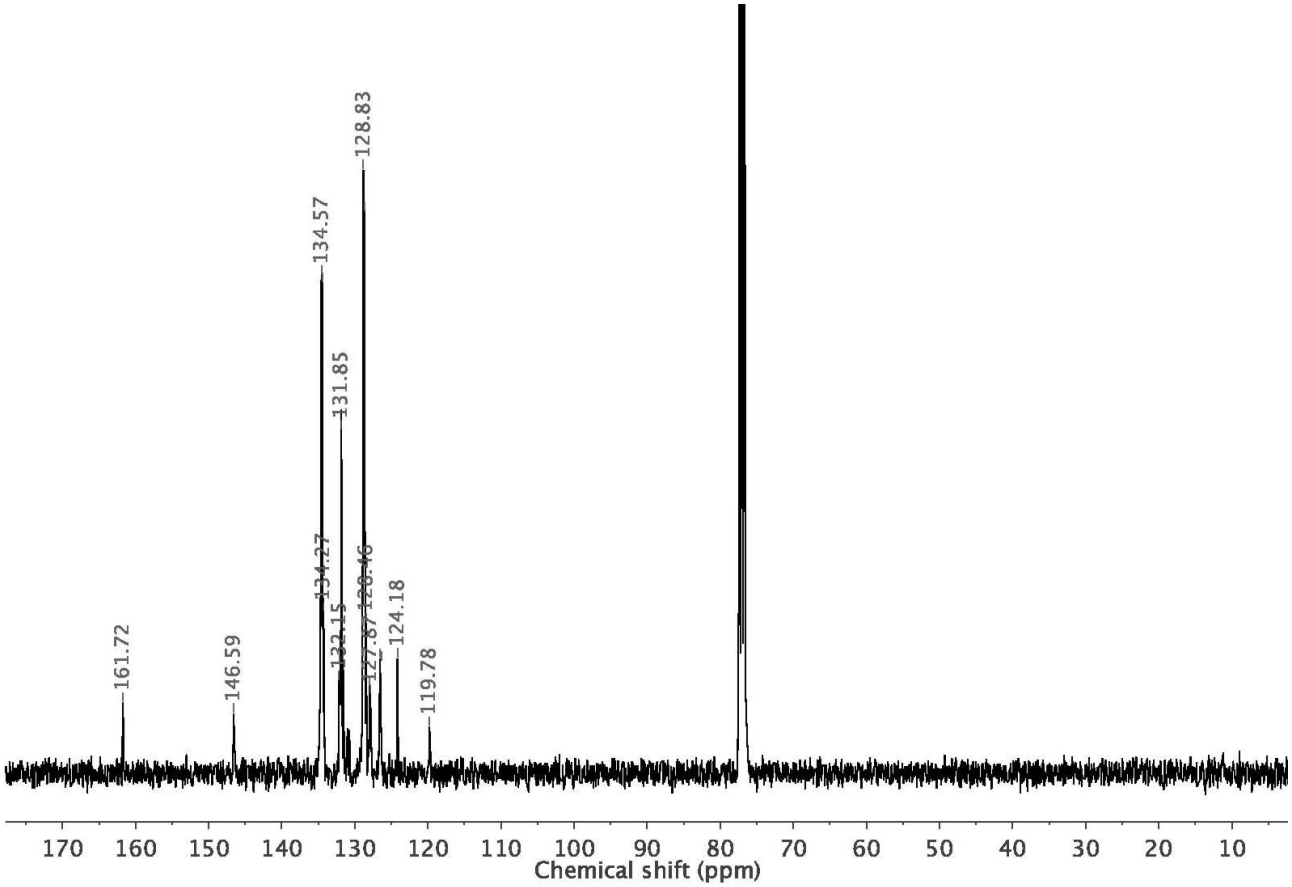


**Figure 19S**. $^{13}C\{^{1}H\}$ NMR spectrum of complex [(μ-diNC-5){$PtCl_2(PPh_3\}_2$] (**5**) in $CDCl_3$.

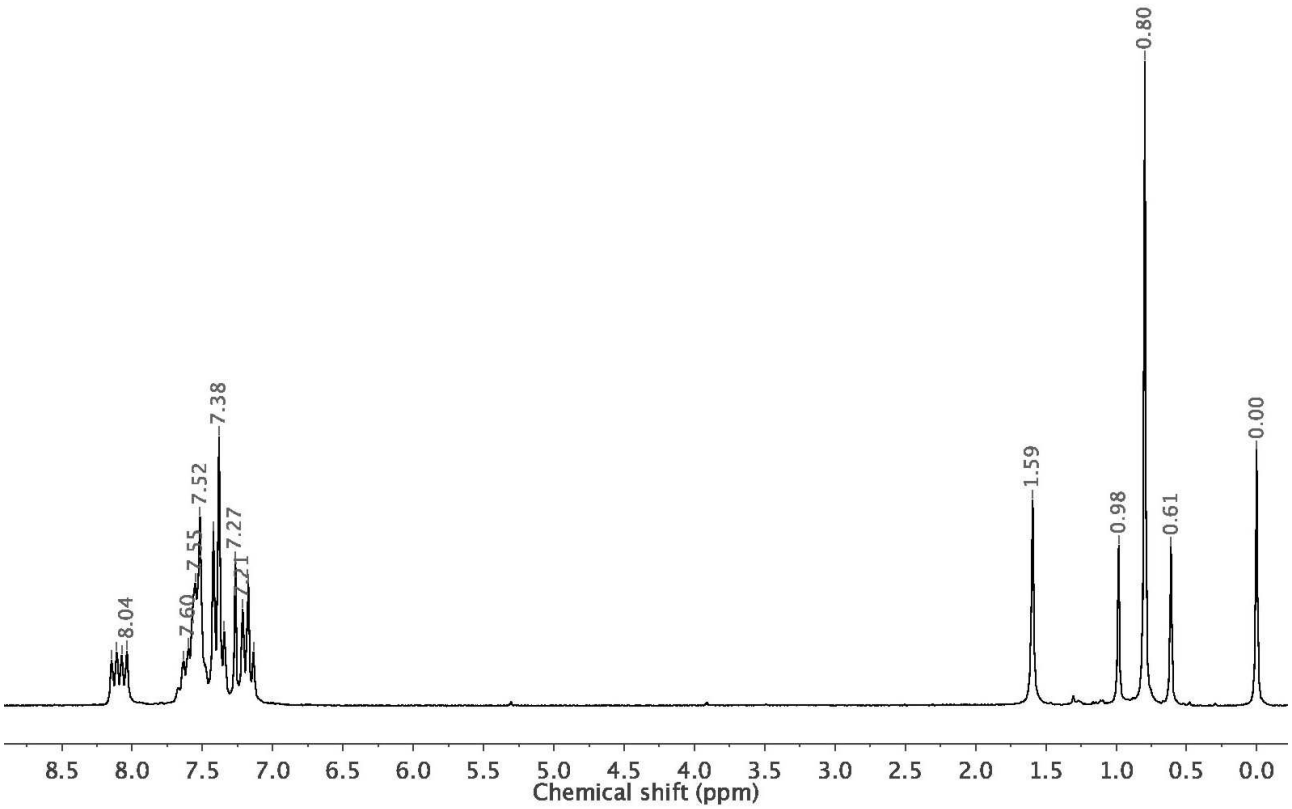


**Figure 20S**. $^{1}H$ NMR spectrum of complex [$PtMe_2$(diNC-1)] (**1'**) in $CDCl_3$.

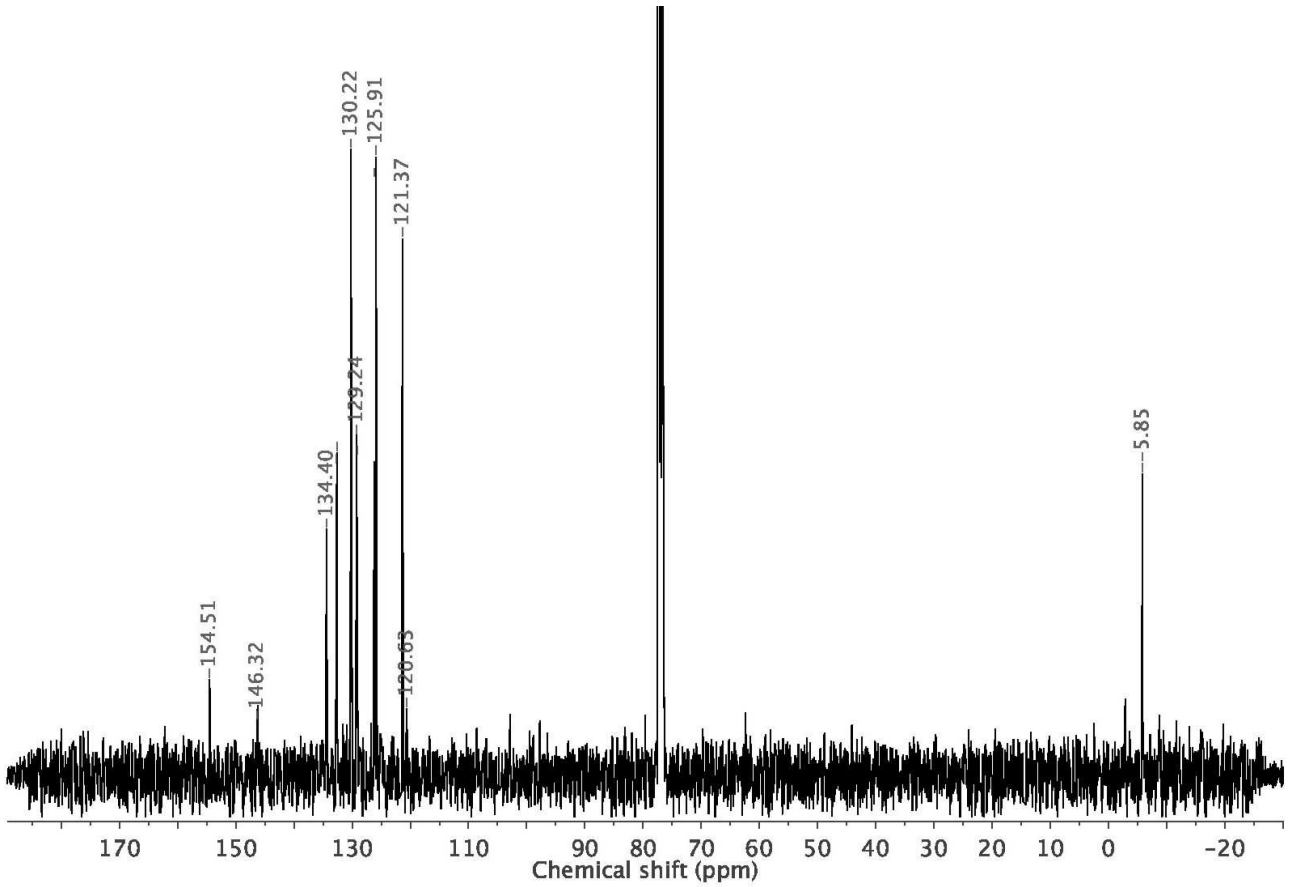


**Figure 21S**. $^{13}C\{^{1}H\}$ NMR spectrum of complex [$PtMe_2$(diNC-1)] (**1'**) in $CDCl_3$.

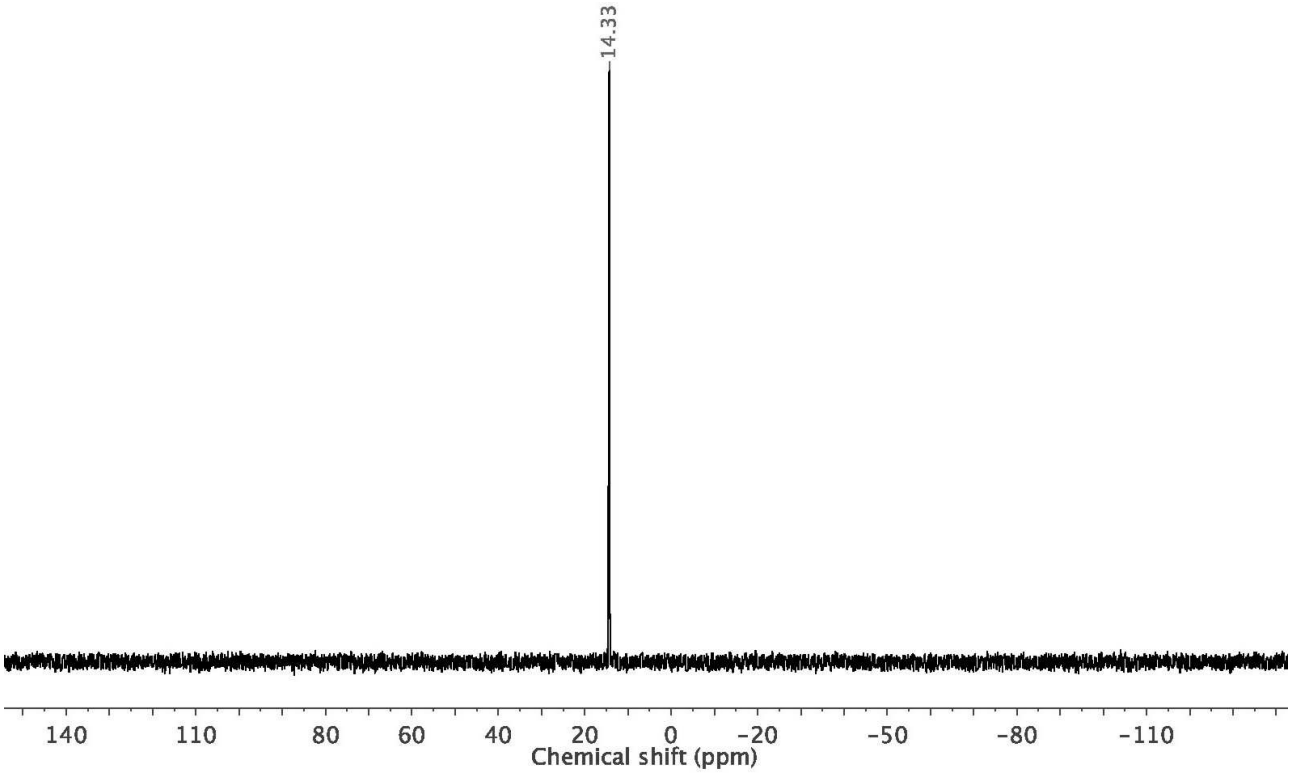


**Figure 22S**. $^{31}P\{^{1}H\}$ NMR spectrum of complex [$PtMe_2$(diNC-1)] (**1'**) in $CDCl_3$.

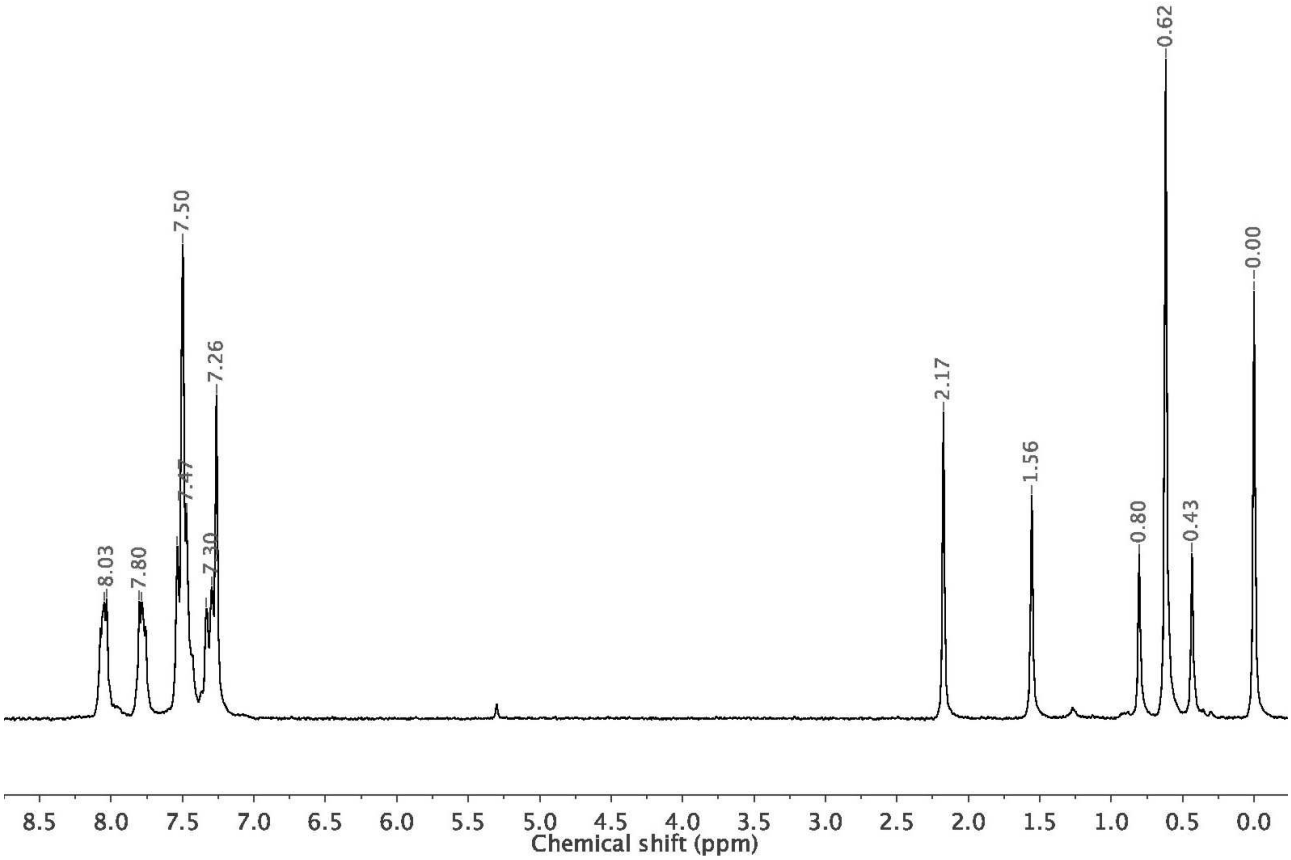


**Figure 23S**. $^{1}H$ NMR spectrum of complex [$PtMe_2$(diNC-2)] (**2'**) in $CDCl_3$.

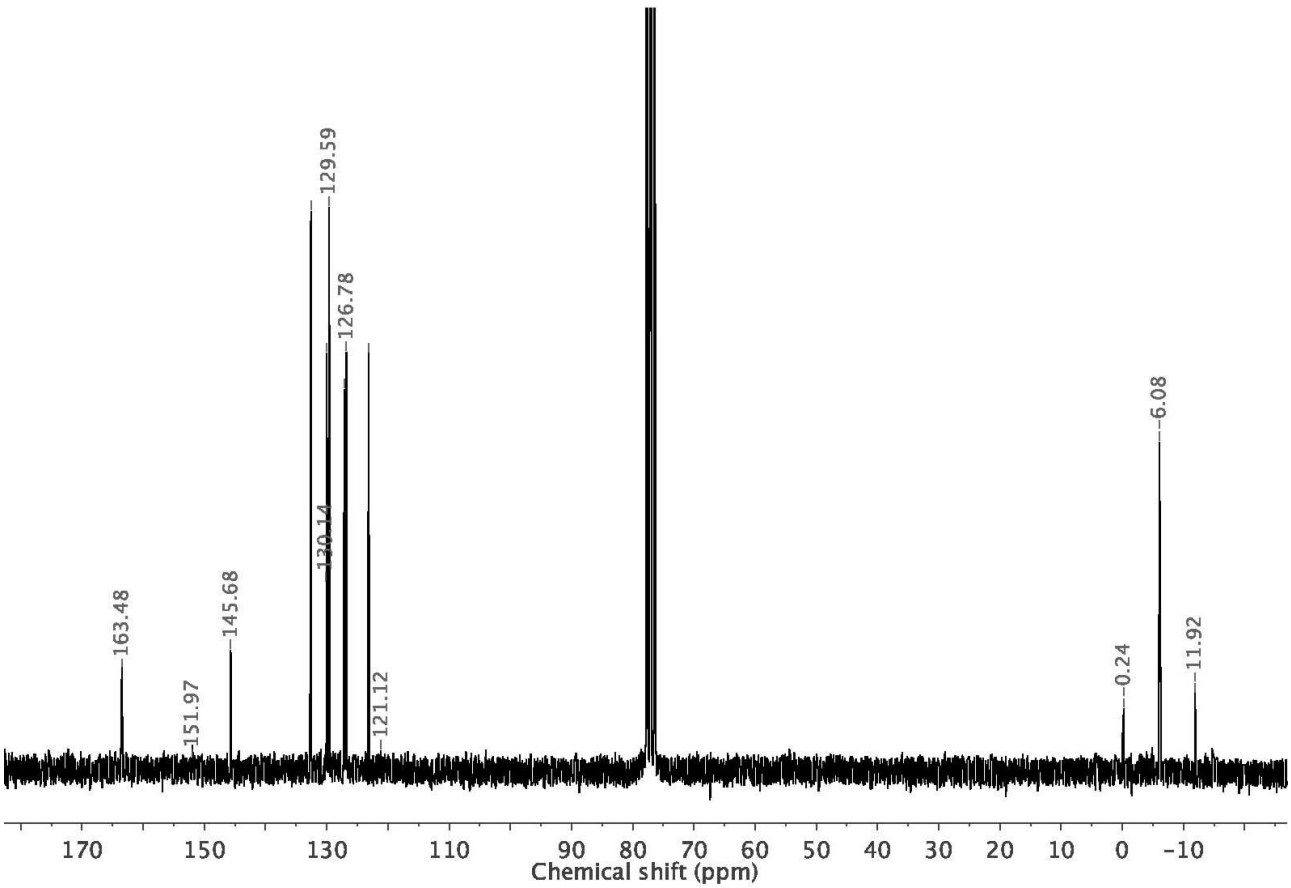


**Figure 24S**. $^{13}C\{^{1}H\}$ NMR spectrum of complex [$PtMe_2$(diNC-2)] (**2'**) in $CDCl_3$.

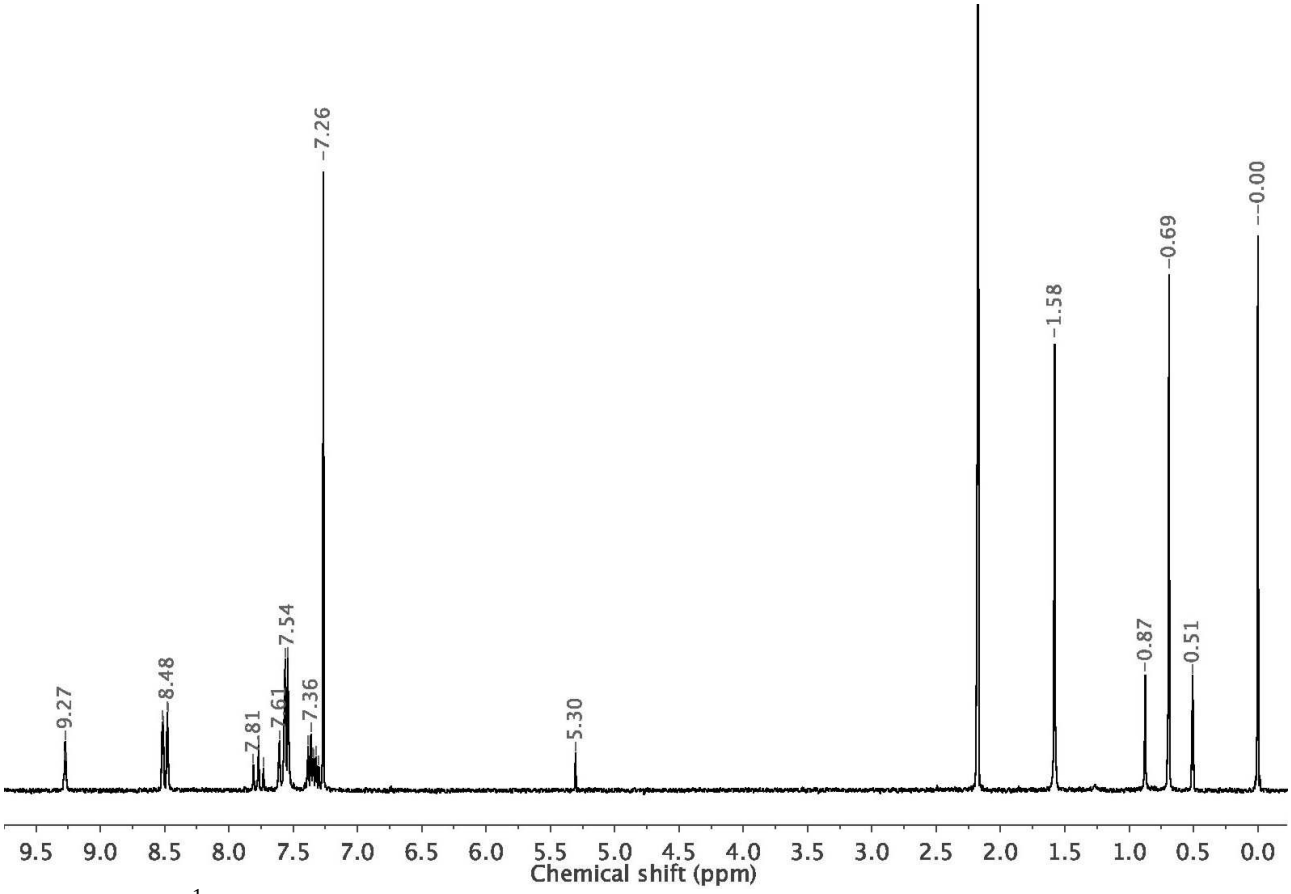


**Figure 25S**. $^{1}H$ NMR spectrum of complex [$PtMe_2$(diNC-3)] (**3'**) in $CDCl_3$.

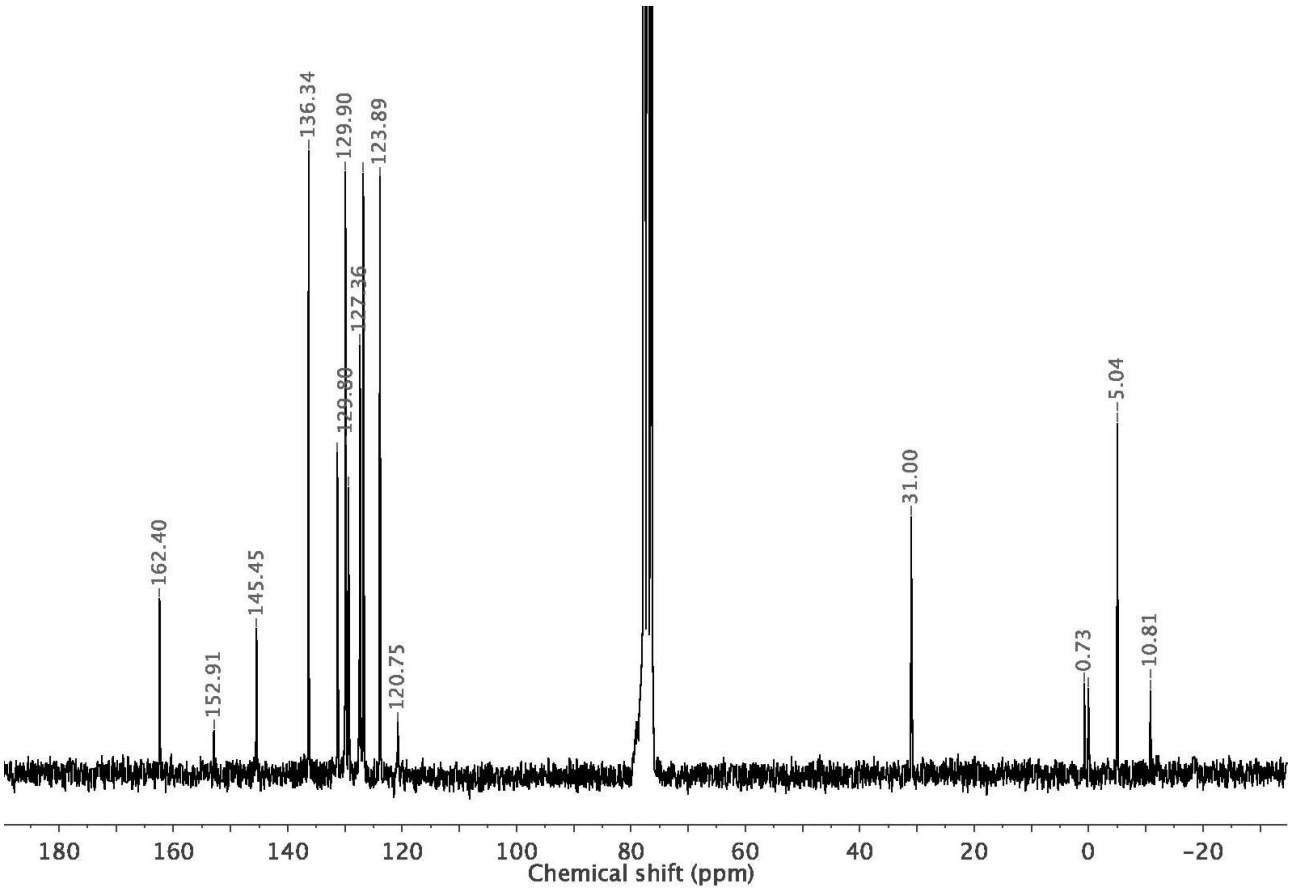


**Figure 26S**. $^{13}C\{^{1}H\}$ NMR spectrum of complex [$PtMe_2$(diNC-3)] (**3'**) in $CDCl_3$.

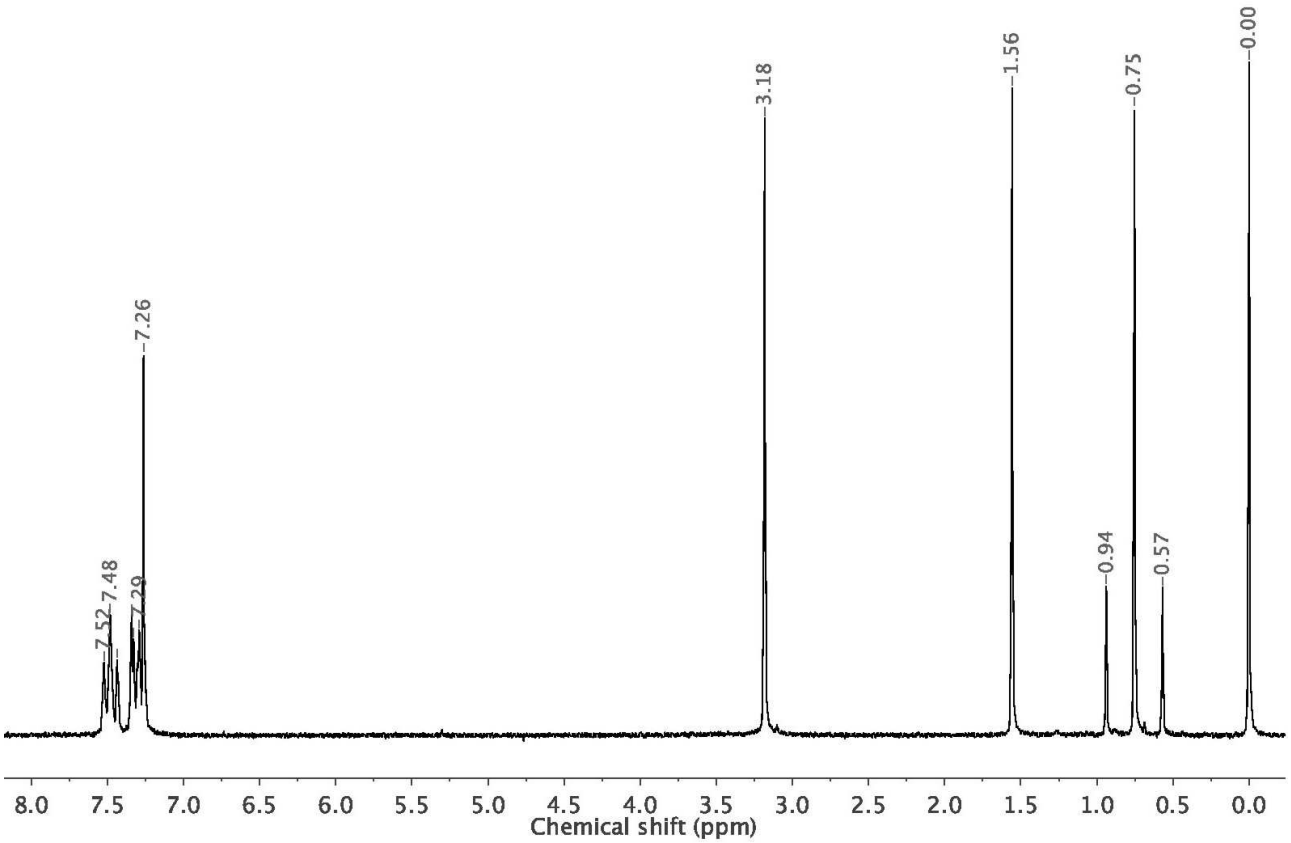


**Figure 27S**. $^{1}H$ NMR spectrum of complex [$PtMe_2$(diNC-4)] (**4'**) in $CDCl_3$.

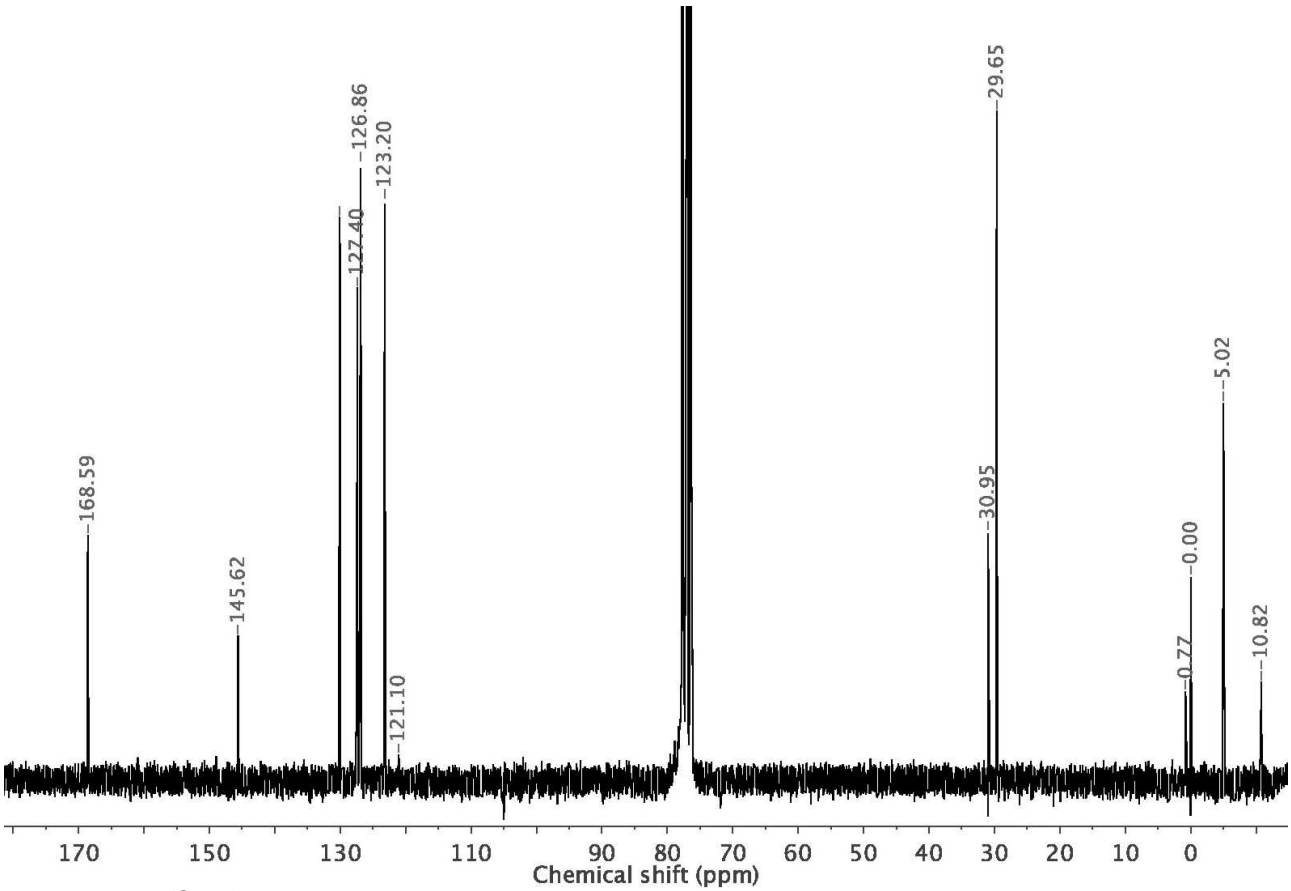


**Figure 26S**. $^{13}C\{^{1}H\}$ NMR spectrum of complex [$PtMe_2$(diNC-4)] (**4'**) in $CDCl_3$.